Experimental Neurology 321 (2019) 113034

Contents lists available at ScienceDirect

Experimental Neurology

journal homepage: www.elsevier.com/locate/yexnr

Research Paper

Demyelination contributes to depression comorbidity in a rat model of chronic epilepsy via dysregulation of Olig2/LINGO-1 and disturbance of calcium homeostasis

Teng Ma, Baichuan Li, Yifan Le, Yang Xu, Fei Wang, Yanping Tian, Qiyan Cai, Zhi Liu, Lan Xiao, Hongli Li*

Department of Histology and Embryology, Army Medical University, Chongqing 400038, China.

ARTICLE INFO

This is the first report to study the connection of myelination disturbance of cerebral white matter and the initiation of depression comorbidity in epilepsy without any application of antiepileptic drugs. Besides, our findings provide a new view understanding the molecular mechanism of depression initiation in epilepsy and also highlighted the importance of myelination situation in psychiatric disorders.

Keywords:
Epilepsy
Depression
Demyelination
Calcium homeostasis
Olig2
LINGO-1

ABSTRACT

Depression is the most common comorbidity among patients with epilepsy. Despite prior assumptions that antiepileptic drugs are to blame, more and more pathological studies have shown that latent neurological alterations associated with white matter injury and demyelination may underlie this link. However, whether disturbances in cerebral myelination contribute to the initiation of depression in epilepsy remains unclear. In the present study, we investigated the connection between demyelination disorders and the development of depression comorbidity in epilepsy. We first induced spontaneous recurrent epilepticus seizure (SRS) in young rats with pilocarpine. We then established depressive behaviors by recurrent forced swimming test and evaluate the depression state by sucrose preference test. The ratio of depression comorbidity in SRS rats was then calculated. Next, myelination in SRS-Depressed (SRS-D) rats was explored via PCR, western blotting, and immunohistochemistry for the key myelin promotion factor, Olig2 and inhibition factor, LINGO-1. Finally, in situ RNA hybridization of NCX3, one of the dominant Ca^{2+} extrusion proteins in oligodendrocytes (OLs) was performed to explore whether Ca^{2+} homeostasis of OLs was disturbed in epilepsy-induced hypoxic conditions and involved in the epilepsy-depression comorbidity. Our results revealed that one-quarter of the SRS rats displayed typical depressive behaviors, which were defined as SRS-D rats. In SRS-D rats, severe demyelination was also observed, accompanied with reduced expression of MBP, Olig2, and NCX3 and increased expression of LINGO-1 in the cingulate gyrus. In SRS-Non depressed rats, no significant changes were found from the control animals. This work provides new insights into the demyelination in epilepsy-depression comorbidity, which involves dysregulation of Olig2/LINGO-1 and disturbance of Ca^{2+} homeostasis.

1. Introduction

Depression is the most common comorbidity in individuals with epilepsy according to clinical research reports (Harden, 2002; Kanner et al., 2012; Mendez et al., 1986). Population-based studies have reported a 6 to 30% lifetime prevalence rate of a depressive disorder in individuals with epilepsy, especially among those with chronic temporal lobe epilepsy or refractory epilepsy (Kanner, 2003). For decades, studies aimed at elucidating the mechanism(s) underlying epilepsy-depression comorbidity have concentrated on the application of antiepileptic drugs. These drugs include primidone (Lopez-Gomez et al., 2005), phenobarbital (Barabas and Matthews, 1988), and others, which are known to cause depression symptoms. Thus, one possibility is that depression in epilepsy is induced iatrogenically.

Recent developments in psychopathological research (Kanner et al., 2012; Valente and Busatto, 2013) have revealed that patients with epilepsy or depression share some common neurological alterations in cerebral white matter (Kavanaugh et al., 2017). For instance, post-mortem pathological assessments of suicide victims with depression have revealed severe white matter demyelination in these individuals

Abbreviations: SE, status epilepticus; SRS, spontaneous recurrent epilepticus seizure; OLs, oligodendrocytes; OPCs, OL progenitor cells; NCX3, sodium/calcium exchanger; MBP, myelin basic protein; EPM, elevated plus maze test; FST, forced swimming test; SPT, sucrose preference test; RT, room temperature; CC, callosum corpus; CG, cingulated gyrus; SRS-EPM^+, SRS-EPM positive rats; SRS-FST^+, SRS-FST positive rats; SRS-EPM^+/FST^+, SRS-both EPM and FST positive rats; SRS-EPM^+/FST^-, SRS-EPM positive and FST negative rats; SRS- FST^+/EPM^-, SRS-FST positive and EPM negative rats; SRS-FST^-/EPM^-, SRS-both EPM and FST negative rats; SRS-D, SRS-Depressed rats; SRS-ND, SRS-None depressed rats.

* Corresponding author at: Department of Histology and Embryology, Army Medical University, Chongqing 400038, China.
E-mail address: lihongli@tmmu.edu.cn (H. Li).

https://doi.org/10.1016/j.expneurol.2019.113034
Received 14 March 2019; Received in revised form 30 July 2019; Accepted 11 August 2019
Available online 12 August 2019
0014-4886/

(Tham et al., 2011). Additionally, the cells responsible for myelination in the CNS-oligodendrocytes (OLs)- exhibited dysfunction and decreased cell density in these tissues (Rajkowska et al., 2015). In patients with epilepsy, abnormal neuronal discharge has also been found to induce hypoxia, which directly inhibits the differentiation of OLs (Hu et al., 2016; Yuen et al., 2014). Together, these prior studies indicate that epilepsy-depression comorbidity may be associated with latent pathological changes associated with demyelination, resulting in brain function disturbances and the potential initiation of psychiatric disorders. Despite this compelling hypothesis, few reports have directly assessed this hypothetical mechanism.

Myelination in the CNS is regulated by various factors via a complicated signal network (Baumann and Phamdinh, 2001). The transcription factor Olig2 plays a critical role in promoting myelination (Yu et al., 2013) and has been reported to accelerates the process of myelin sheath formation and remyelination (Ligon et al., 2006; Mei et al., 2013). Conversely, abnormal downregulation of Olig2 contributes to demyelination processes and depression (Aston et al., 2005; Benner et al., 2016; Hae-Chul et al., 2015).

Despite Olig2's crucial, positive effects on myelination, recent studies have also reported that myelination is regulated by the LINGO-1 protein via negative inhibition (Jepson et al., 2012). LINGO-1 serves as a transmembrane protein, which is selectively expressed on the plasma membrane of neurons and OLs (Llorens et al., 2010). Under normal conditions, expression of LINGO-1 by neurons or OLs restricts OL differentiation and myelination (Lee et al., 2007). However, in pathological conditions, such as: multiple sclerosis, LINGO-1 expression was significantly increased in OL progenitor cells (OPCs) from demyelinated white matter (Mi et al., 2013). Thus, negative functional regulation of myelination process via LINGO-1 may serve as a potent actor in demyelination injuries. In summary, myelination processes in the CNS are regulated by two key factors, Olig2 and LINGO-1, which exhibit facilitation and inhibition effects on myelination, respectively. However, to date, whether dysregulation of Olig2 or LINGO-1 serves as the pivotal molecular mechanism in the initiation of demyelination and are induced with psychiatric disorders remains unclear.

Ca^{2+} signals play an indispensable role in the development of OLs. Intracellular Ca^{2+} alterations not only interfere with the transition of OPCs into mature myelinating OLs, but also intervene in the initiation of myelination and remyelination processes (Soliven, 2001). In epilepsy patients, seizures exacerbate ischemic-hypoxic injuries in the brain (Szebeni et al., 2014). Overaccumulation of oxidative stress factors with hypoxia also interferes with the expression of Ca^{2+} extrusion proteins (Kip and Strehler, 2007). Our previous work has found that NCX3 (sodium/calcium exchanger), a dominant Ca^{2+} plasma membrane extrusion protein, induces Ca^{2+} overload injuries in OPCs when NCX3 expression is inhibited by hypoxic conditions (Ma et al., 2015). Therefore, NCX3 expression in OLs serves as a marker of Ca^{2+} homeostasis disturbances and injury in OLs.

In the present study, we used lithium chloride pilocarpine to induce spontaneous recurrent epileptic seizures (SRS) in young rats. We then used recurrent forced swimming test (FST) to induce the onset of depressive behaviors and sucrose preference test (SPT) to evaluate depression state in SRS rats. We further assessed demyelination via the expression of Olig2, LINGO-1, and NCX3 in SRS-Depressed (SRS-D) rats. Our results suggest that pilocarpine successfully induced SRS behaviors in rats and that among SRS rats, one quarter displayed depression comorbidity, which were defined as SRS-D rats (8/32). In SRS-D rats, demyelination was also evident, as well was reduced expression of myelin basic protein (MBP). Alterations in Olig2, LINGO-1, and NCX3 expression were also confirmed in white matter regions. In SRS-Non depressed (SRS-ND) rats (24/32), we did not find significant changes relative to controls. In conclusion, this work provides valuable new insights into the mechanisms underlying epilepsy-depression comorbidity, suggesting that dysregulation of Olig2/LINGO-1 and disturbance of Ca^{2+} homeostasis contribute to demyelination. The molecular mechanism may play an important role in the initiation of epilepsy-depression comorbidity.

2. Materials and methods

2.1. Animals

All male Sprague-Dawley rats (3 weeks old, 70 ± 5 g) were procured from the Animal Facility Center of the Third Military Medical University (Chongqing, PR China). Rats were individually housed in a controlled environment (22 ± 1 °C; humidity: 60%; lights on from 07:00–19:00) with ad libitum access to food and water. All procedures were performed in accordance with the protocols set and approved by the University Committee on Animal Care and Use. A total of 50 rats were procured of which 40 were used in the experimental group and 10 in the normal control group.

2.2. Experiment time line and rat's allocation

At postnatal 21 d, status epilepticus (SE) was induced by pilocarpine injection in SD rats. 12 weeks later, SRS state was evaluated by EEG recording and daily behavior observation (3:00–4:00 pm, 1 continuous hour for 7 d). Then, the depression state was induced by FST (every 3 d and totally for 3 weeks) and evaluated by SPT. After establishment of epilepsy-depression comorbidity model, rats were sacrificed for following experiments.

As shown in Fig. 1, 10 rats were distributed to normal control group. After SE state was established in 40 rats, 32 rats entered SRS state. In behavior test, only 25% of SRS rat, which were both positive for elevated plus maze test (EPM) and FST (SRS-EPM^+/FST^+ group) displayed SPT-positive result and were distributed to SRS-depressed group (SRS-D, n = 8). The rest 75% of SRS rats, due to negative results of SPT, were allocated to SRS-None depressed group (SRS-ND, n = 24). Details were presented in following parts.

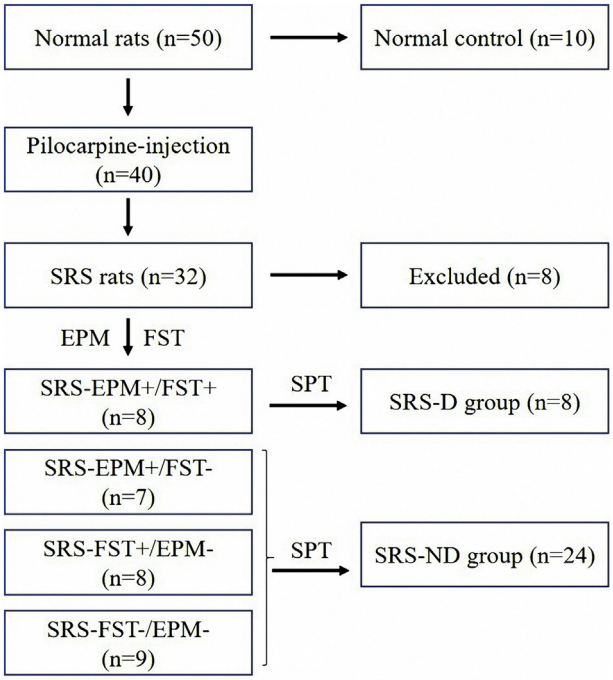

Fig. 1. Flow chart of rat's allocation. 10 rats were distributed to normal control group. Among 32 SRS rats, 8 rats with SRS-EPM^+/FST^+ phenotype were defined as SRS-D group while the rest 24 SRS rats were allocated to SRS-ND group.

2.3. Seizure induction

Pilocarpine hydrochloride (380 mg/kg, Sigma) was dissolved in 0.9% saline and 30 mg/kg was injected intraperitoneally (i.p.), as has been done previously to induce seizures (Faure et al., 2013). Lithium (127 mg/kg in 0.9% saline) was administered i.p. 30 mins prior to pilocarpine administration to minimize pilocarpine's peripheral effects. The animals were monitored throughout SE induction and seizure severity was assessed according to a modified Racine's scale (Racine et al., 1972). Motor seizure activity was characterized as follows: class I as hypoactivity, mouth and facial automatism; class II as head nodding and mastication; class III as forelimb clonus with a lordotic posture; class IV as rearing with concomitant forelimb clonus; and class V as generalized clonic convulsions and loss of balance. When no clear behavioral changes were observed within 1 h of injection, additional pilocarpine injections (5 mg/kg) were administered each hour until a clear change in behavior was induced. An SE was considered to have been established if rats experienced more than two stages and entered IV or V seizure stage within the first hour after the last injection. Control rats were injected intraperitoneally with 0.9% saline. After successful induction, no more pilocarpine injections were performed.

2.4. EEG recordings

To record the spread of electrographic seizure activity to the ipsilateral hippocampus or the contralateral cortex, a recording cable was connected to the EEG electrode and the resulting signal was amplified (500–5000 times) and filtered (1–30 Hz) (Neurolog System: NL 824, remote pre-amplifier; NL 820, isolated amplifier; NL 135, low-pass filter; NL 530 conditioner; Digitimer Ltd., Welwyn Garden City, UK) prior to being displayed on an oscilloscope and recorded on chart paper. A bipolar electrode was implanted into the hippocampal hilus (distance between the tips 0.8 mm; coordinates of the lower tip: 4.1 mm posterior, 2.6 mm lateral and 3.7 mm ventral to bregma) and a screw electrode (Plastics One Inc., Roanoke, VA) was attached to the skull overlying the contralateral frontal cortex (coordinates: 3.0 mm anterior and 2.0 mm lateral to bregma). Two monopolar stainless steel screw-electrodes that were fixed to the skull symmetrically over the cerebellum with dental acrylate (Selectaplus CN, Dentsply DeTrey GmbH, Dreieich, Germany) served as to ground the reference electrodes. Spectra were continuously acquired, displayed, and stored.

2.5. Establishment and evaluation of depression state in rats

It's reported that single pilocarpine injection directly induced long-term anxiety behaviors in rats (Duarte et al., 2013). The early onset of anxiety disorder accelerated the onset of major depression disorders and increased the severity (Fava et al., 2000; Schaffer et al., 2000). Thus, we performed EPM to evaluate the secondary anxiety situations in pilocarpine-induced SRS rats.

EPM: devices (BW-DEP 207, Shanghai Bio-will Co., Ltd) were made of wood which was painted dark grey and comprised of two open, opposing arms (70 cm × 12 cm), and two closed, opposing arms (70 cm × 12 cm with 17 cm high walls) arranged in a cross shape. Devices were raised on the scaffold, 80 cm above the floor. A central square region served to connect the arms (10 cm × 10 cm). During testing, each animal was placed into the central region, positioned to face an open arm. Behavior was recorded over a 10-min period via a video recorder mounted above the maze. Animal tracking software ('Tracker' University of Edinburgh) was used to calculate the duration of time each animal spent in each arm and in the central region of the maze. The apparatus was wiped clean with ethanol between animals. The total entries were calculated to display the motor capability. The amount of time rats spent in the open versus that in the closed arms (mins spent on the central square) was compared. The percentage of open arm entry was measured.

After EPM test, despair behaviors and psychological stress was induced by FST to establish the comorbid depression. FST: FST was performed according to a previously optimized protocol (Porsolt et al., 2011). Briefly, rats were placed in transparent plastic cylinders (BW-DFS 201, Shanghai Bio-will Co., Ltd., 10 cm diameter, 30 cm height) containing 20 cm^3 of water at 24–26 °C. Rats were left in the cylinder for 8 min and their behavior was recorded. In the first 4 min, rats were forced to swim so that they gradually got used to FST situation then in the following 4 min, time spent immobile was measured. FSTs were performed every 3 d and the mean immobility time from trials were calculated as the final results.

After depressive behaviors was induced by FST, the evaluation of depression state and severity was determined by anhedonia situations in rats. That's SPT: The adaptation training of sucrose water intake was performed before experiment initiation. Two water bottles were prepared for each cage. During the first 24 h period, both water bottles were filled with 1% sucrose water. During the following 24 h period, one bottle was filled with 1% sucrose water and the other one was replaced by pure water. After fasting and water deprivation for 12 h, each cage was provided with two bottles at the same time, one bottle was 1% sucrose water, and the other one was pure water. After 1 h, two bottles were collected and weighed. The preference rate of sucrose water = (sucrose water consumption/total liquid consumption) $_*$ 100%.

Before rat brain tissues were collected for different experiments, the extra western blot analysis of depression marker was also performed. In major depression, the level of inflammatory cytokines, like: IL-1β, CRP, IL-6, etc. (Lopresti et al., 2014), were closely associated with depression state, but it was not specific. Western blot analysis of IL-1β (details see below) expression in the white matter were performed as the secondary evidence to support the evaluation of depression state in rats.

2.6. RT-PCR

Total RNA from homogenized rat brain tissue was collected using Trizol (Life Technology, USA), according to the manufacturer's instructions. The 260/280 value was strictly controlled at 1.9–2.0 to ensure the high purity of RNA. Single-stranded cDNA was synthesized from total RNA using oligo-dT primers and Super scriptase III enzyme (Life Technology, USA). The specific primers sequences were listed: Olig2 forward sequence: 5′-CGGGAATTCTAG-ATCGTCTCCGGGGC CAT-3′; Olig2 reverse sequence: 5′-GGGGTACCATCTT-GGCGTCGGAG GTGAG-3′; LINGO-1 forward sequence: 5′-AACCTGGAGACGCTCA TTC-3′; LINGO-1 reverse sequence: 5′-CTGCTGCCTGTTGAAGTTG-3′; β-actin forward sequence: 5′-CGTTGACATCCGTAAAGACC-3′; β-actin reverse sequence: 5′-CATCGTACTCCTGCTTGCT-3′.

All PCR reactions were performed using a programmed cycle (94 °C, 30 s; 55 °C, 30 s, and 72 °C, 1 min for 30–35 cycles). The optical density of the bands of PCR products (normalized to actin) were determined via the Image-Pro Plus image analysis system.

2.7. LFB staining

Rat brain tissues were fixed by 4% paraformaldehyde in PBS and sliced into sections. Sections were soaked in 0.1% LFB (Sigma solution for myelin staining at 60 °C overnight, followed by dye removal in non-white matter tissues) using 95% ethanol, 0.05% lithium carbonate solution, 70% ethanol, and distilled water. Sections were then soaked in ethanol followed by xylene for dehydration and transparency. Images were taken at 400× magnification with a light microscope (Olympus AX-70) and analyzed via Image Tool 2 software (Olympus, Japan).

2.8. Immunohistochemistry and Nissl staining

For immunohistochemical staining, brain sections were treated with 0.3% hydrogen peroxide in methanol for 15 min then washed with

0.01 M PBS and incubated with a blocking solution composed of 0.3% Triton X-100 and 5% BSA in PBS at room temperature (RT) for 1 h. The same solution was used for the primary antibody solution, in which tissues were incubated overnight at 4 °C. The following primary antibodies were used: MBP (mouse monoclonal; 1:200; Santa Cruz Biotechnology, CA); Olig2 (rabbit monoclonal; 1:200; Abcam, USA); LINGO-1 (rabbit polyclonal; 1:200; Abcam, USA). Tissue sections were incubated for 2 h with alpaca anti rabbit 488 (1:200; Jackson, USA) and Goat anti rabbit TRITC (1:200; Boster, China) for immunofluorescence, as well as with horseradish peroxidase-linked secondary antibodies (1:200, Santa Cruz) at RT for immunoenzymes. Following PBS rinses for 3 times, antigen-antibody complexes were visualized using DAB (Boster, China) as the chromogen. Tissues were imaged for immunoreactivity with a confocal laser-scanning microscope (Olympus IX81, Japan).

For Nissl staining, 10 μm-thick sections were mounted directly onto gelatin-coated glass slides and air-dried. Slides were then stained with 1.0% cresyl violet, dehydrated, and cover slipped with Entellan (Beyotime, China). The number of the CA1 pyramidal cells in the hippocampus in stained sections (three sections of hippocampus for each rat between levels 2/3 and 5 mm posterior to the bregma fortune) were counted at 400× magnification with a light microscope by a blind investigator. Only cells with an evident nucleus and nucleolus were included. Images were taken at 400× magnification with a microscope (Olympus AX-70) and analyzed via Image Tool 2 software (Olympus, Japan).

2.9. Western blot analysis

For western blot analysis, samples (tissue and cultured cells) were extracted using a RIPA lysis buffer with freshly prepared 1% PMSF solution (Biocolors, China). After protein determination using Coomassie brilliant blue G250, samples were denatured and separated on SDS-PAGE gels. Following electrophoresis, proteins were transferred to polyvinyldifluoride membranes. These membranes were incubated overnight at 4 °C with the primary antibodies (1:1000) and then incubated with HRP-linked secondary antibodies (1:2000–3000, Santa Cruz). Immunoreactive bands were detected using an ECL plus detection kit (ECL plus, GE Healthcare). The optical density of the bands (normalized to those for actin) was determined with the Image-Pro Plus image analysis system.

2.10. Electron microscopy

Specimens were collected, sectioned (2 mm × 2 mm × 1 mm), and fixed in 2.5% phosphate-buffered glutaraldehyde for 24 h. They were then individually placed into 1% osmium tetroxide and gradients of 25%, 50%, 75%, and 95% ethanol, propylene oxide, and embedded in a 50:50 mixture of propylene oxide and araldite resin as well as 100% araldite. These blocks were then shaken and then evacuated to remove propylene oxide and oven dried at 60.1 °C for 24 h. After sectioning, all blocks were stained with uranyl acetate and lead citrate for 10 min each and then examined at 70 kV on a Philips EM 208 electron microscope (Philips, Eindhoven, Netherlands). Images were obtained on an AMT XR50 digital imaging system (Advanced Microscopy Techniques, Woburn, MA, USA).

2.11. In situ RNA hybridization

A NCX3-DIG (Digoxigenin) labeled RNA probe in situ hybridization kit (Boster, China) was used. Tissue preparation and in situ hybridization were performed according to Schaeren-Wiemers and Gerfinmoser (Schaerenwiemers and Gerfinmoser, 1993) with some minor modifications. Briefly, brain sections were fixed in 4% paraformaldehyde at 4 °C overnight and then digested with proteinase K (10 μg/mL) in PBS for 5 min, washed with PBS-T, and finally hybridized with antisense-oligonucleotides RNA probes in hybridization buffer (50% formamide, 10% dextran, 5× SSC, 0.1% Tween, 1 mg/mL yeast RNA, 100 g/mL heparin, 1× Denhardt's, 0.1% CHAPS, 5 mM EDTA) at a concentration of 1 μg/mL for at least 16 h at 42 °C. Sense oligonucleotides RNA probes and only hybridization buffer (no probes) were used as negative controls. After thorough washing in 4 × SSC, 2 × SSC, 1 × SSC, 0.5 × SSC, and PBS-T (twice for 10 min), sections were incubated for 1 h with anti-DIG-Fab-AP (1:1000) conjugate and washed in PBS-T. Finally, the sections were incubated with a 5-bromo-4-chloro-3-indolyl phosphate/nitro blue tetrazolium liquid substrate system. Color development was stopped after 30 min at RT. Positive results in the slices were indicated by a blue stain. No blue signals were observed in negative control slices.

2.12. Quantitative image analyses

For stereological quantification, serial brain coronal sections containing the callosum corpus (CC) and cingulated gyrus (CG) were collected (about 50 sections) and 10 sections were sampled from each animal in a systematic and random manner. For statistical analyses, at least nine representative fields were randomly acquired at 20× magnification from each of the two experiments (performed in triplicate). Cell counting was conducted on nine randomly chosen fields in each sample (Media Cybernetics, Silver Spring, MD). Quantification of immunostaining and cell counting was performed using Image-Pro Plus. The optical density of the bands of PCR products or western blot results (normalized to those of β-actin) were also determined by the Image-Pro Plus image analysis system (Media Cybernetics, Silver Spring, MD, USA).

2.13. Statistical analyses

Data are expressed as mean ± SD for each treatment group. Statistical analyses were performed using one-way ANOVAs, followed by Tukey's post-hoc test. Comparisons between the two experimental groups were made using a student's *t*-test. Statistical analyses were performed using SPSS 16.0. Differences were considered to be statistically significant with a $p < .05$.

3. Results

3.1. The SRS rat model was successfully established after a pilocarpine treatment-induced acute SE state

To evaluate whether SE was induced in the rat cerebrum after intraperitoneal injection of pilocarpine (30 mg/kg), EEG and Nissl staining were performed to assess cerebrum physiology and morphology. As shown in Fig. 2A, B, EEG revealed that the normal control group assumed basic α and β rhythms with steady fluctuations. However, pilocarpine-treated rats exhibited representative epileptic waves. These waves included recurrent sharp waves, spikes, slow waves, sharp and slow comprehensive waves. Nissl staining revealed that compared with control group, neurons in pilocarpine-treated SE rats were arranged loosely, with fuzzy contours, and unclear color and flash (Fig. 2D, E). After SE, to evaluate whether SE rats developed chronic epilepsy (SRS), we used behavioral inclusion criteria. Assessed behaviors included falling, convulsions, recurrent spontaneous forelimb clonus, tonic-clonic movement(s) of the limbs, loss of balance, facial myoclonus, and others. All behaviors were recorded. If behaviors were recorded more than three times within 7 d, the rat was determined to belong to the SRS group. Our results revealed that, among a total of 40 rats, 32 developed SRS with different types of behaviors (80%, Fig. 2F). EEGs of the SRS rats reveal small scale fluctuations, which were steady and differed from those of normal and SE group animals (Fig. 2C). This suggests that pilocarpine treatment directly induced SE following SRS in the rat cerebrum.

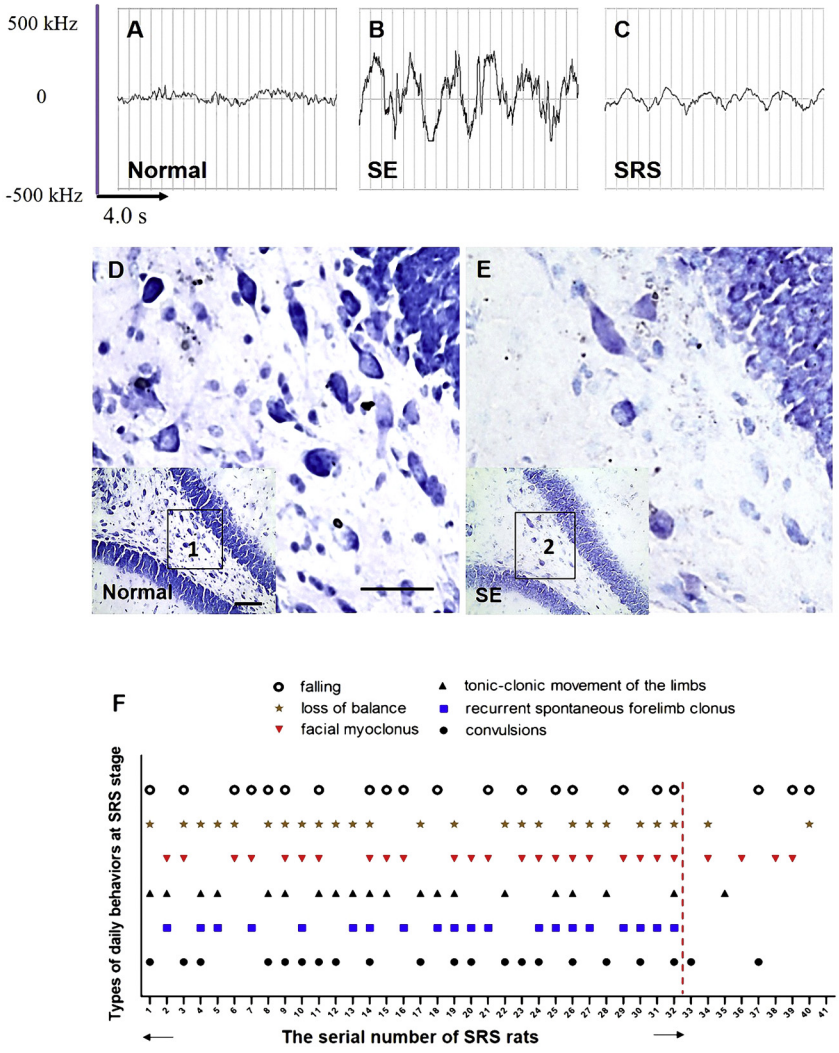

Fig. 2. A. B. C: EEG results of normal, SE and SRS group: normal control group took the α, β wave as the basic rhythm with steady fluctuation; SE group showed representative epileptic waves: recurrent sharp waves, spikes, slow waves, sharp and slow comprehensive waves; SRS group showed small scale fluctuation, which was steady and different from the control and SE group. D.E: Nissl staining revealed that compared with control group, neurons in pilocarpine-treated SE rats were arranged loosely, with fuzzy contours, and unclear color and flash. Scale bar = 50 μm. F: Among 40 rats, 32 SRS rats presented more than three times of epileptic behaviors within a week: falling, convulsions, recurrent spontaneous forelimb clonus, tonic-clonic movement of the limbs, loss of balance, facial myoclonus, etc.

3.2. Comorbid depression was established in approximately one quarter of all SRS rats

To induce the onset of comorbid depression in SRS rats, behavior tests were combined to establish the depressive behaviors and evaluate the depression state. Firstly, as the anxiety-like response was always induced by pilocarpine injection and anxiety state correlated tightly with the onset and severity of depression disorder. EPM was performed to evaluate the anxiety situations 12 weeks after pilocarpine injection in SRS rats. Result displayed that compared with normal group, 47% SRS rats exhibited EPM positive phenotypes (SRS-EPM$^+$) while 53% SRS rats exhibited negative phenotypes (SRS-EPM$^-$). SRS-EPM$^+$ group displayed significantly decreased open arm time and decreased percentage of open arm entry in the EPM when compared to normal or SRS-EPM$^-$ groups ($p < .05$, Fig. 3A, B). However, these was no significant differences of total entries among groups (Fig. 3C), indicating motor capabilities of SRS rats were not affected.

Then, FST was performed every 3 d and totally 3 weeks to induce the despair behaviors and psychological stress in SRS rats. Result displayed that compared with normal group, 50% SRS rats exhibited FST positive phenotypes (SRS-FST$^+$) with increased immobility time ($p < .05$, Fig. 3D). Combining FST and EPM results, SRS rats were divided in four groups with distinct behavior phenotypes: SRS-EPM$^+$/FST$^+$($n = 8$); SRS-EPM$^+$/FST$^-$($n = 7$); SRS-FST$^+$/EPM$^-$($n = 8$); SRS-FST$^-$/EPM$^-$($n = 9$) (Fig. 3E). Finally, the crucial depressive factor, anhedonia, was evaluated by SPT to determine depression state among groups. Result displayed that compared with normal group, the preference rate of sucrose water was only significantly decreased in SRS-EPM$^+$/FST$^+$ group ($p < .05$, Fig. 3F). It indicates that severe depression disorder was only established in the SRS rats with preceded anxiety disorder. The early onset of anxiety in SRS rats deteriorated depressive phenotypes. SRS-EPM$^+$/FST$^+$ group was then defined as SRS-D group (8/32). SRS-EMP$^+$/FST$^-$, SRS- FST$^+$/EPM$^-$ and SRS- FST$^-$/EPM$^-$ were distributed to SRS-ND group (24/32).

Before rat tissues were collected and prepared for following experiment, an extra western blot analysis of depression marker, IL-1β was performed. Result displayed that compared with normal or SRS-ND group, SRS-D group displayed the significant increase in the expression of IL-1β ($p < .05$, Fig. 3G, H). Although the increase of IL-1β expression also existed between normal and SRS-ND group, but it was not multi-fold. These results strongly suggest that comorbid depression phenotype was successfully established in one quarter of all SRS rats.

3.3. SRS-depressed rats displayed decreased MBP expression and decreased myelination

To further explore whether myelination disturbances were involved in the initiation of epilepsy-depression comorbidity, myelination in CC and CG regions was detected by LFB and MBP immunohistostaining. LFB results revealed that mean optical density (OD) values significantly decreased in the CC and CG regions of SRS-D group animals compared to normal controls ($p < .05$, Fig. 4A, B). No significant differences in

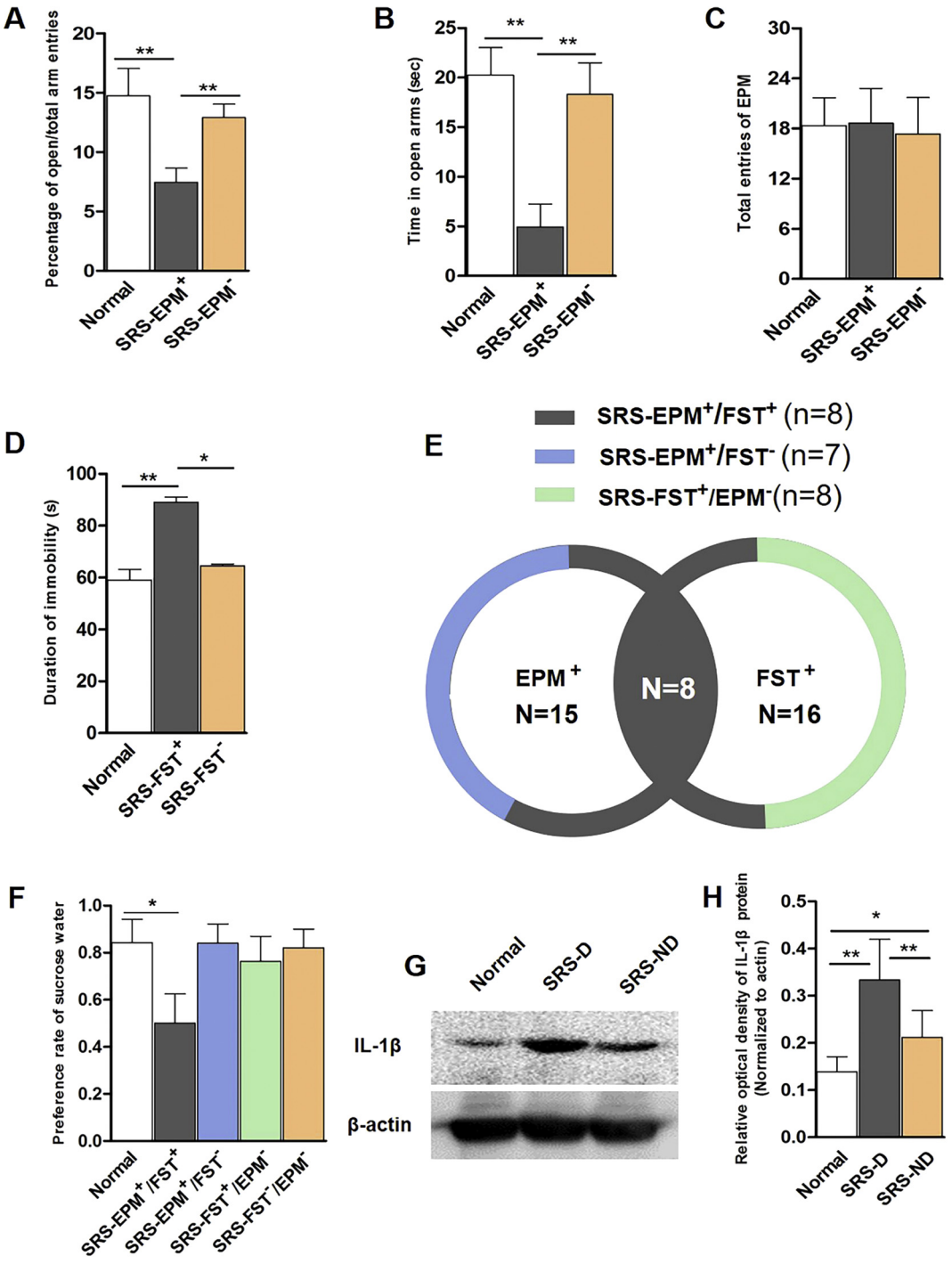

Fig. 3. A: In EPM test, SRS-EPM$^+$ group displayed significant decrease in the percentage of open arm entry and the open arm time (B), compared with normal or SRS-EPM$^-$ group. C: No significant differences of total entries were found in normal and SRS group. D: In FST test, SRS-FST$^+$ group displayed significant increase in the immobility time, compared with normal or SRS-FST$^-$ group. E: Combine EPM and FST results, SRS rats were divided in four groups: SRS-EPM$^+$/FST$^+$; SRS-EPM$^+$/FST$^-$; SRS- FST$^+$/EPM$^-$; SRS- FST$^-$/EPM$^-$. F: In SPT test, significant decrease of preference rate of sucrose water was observed only in SRS-EPM$^+$/FST$^+$. Then, SRS-EPM$^+$/FST$^+$ was defined as SRS-D group (n = 8) and the others were distributed to SRS-ND group (n = 24). F: Western blot showed a multi-fold increase of IL-1β expression in SRS-D group, but not in SRS-ND group. G: elative quantification of western blot results is depicted in the bar graph. The values represent the mean ± SD, * $p < .05$** $p < .01$.

mean OD values were found between SRS-ND rats and normal group animals ($p > .05$). Additionally, the positive intensity of myelin basic protein (MBP) was also markedly reduced in the CC and CG regions in the SRS-D group, a finding which was consistent with our LFB results (Fig. 4A, C). However, the SRS-ND group exhibited similar positive expression of MBP as the normal group in both the CC and CG regions.

Following this, electron microscopy was performed to detect morphological alterations in myelin sheath formation. Our results revealed that, when compared to normal control animals, SRS-D rats exhibited myelin degradation and thinning (Fig. 5A). Statistical analysis showed the percentage of myelinated axons significantly decreased while G-ration was increased in SRS-D group (Fig. 5B, C). Western blot analysis revealed significantly decreased expression of MBP and CNPase but significantly increased levels of GFAP (an astrocytic marker) and

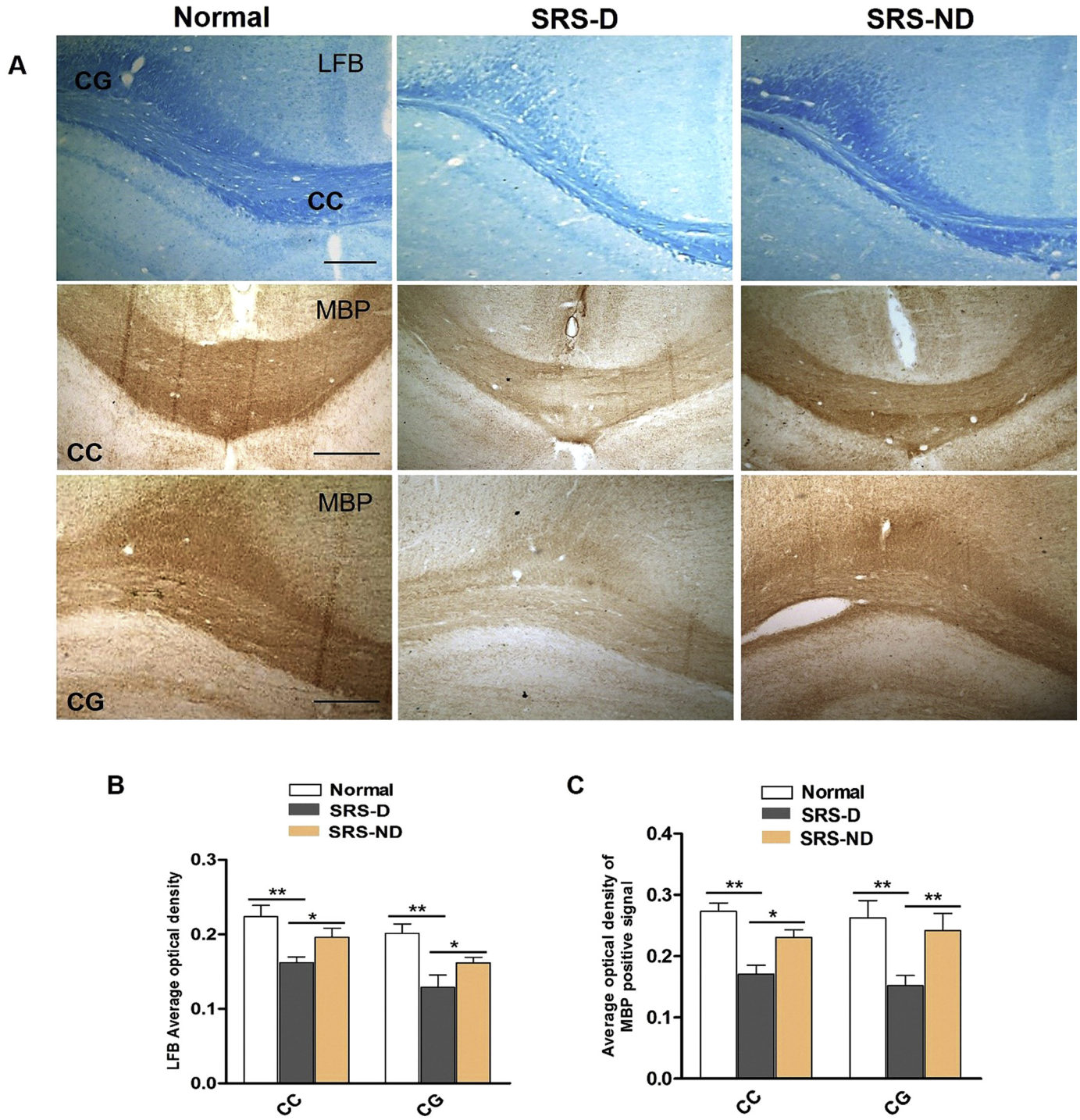

Fig. 4. A: LFB results showed that the mean OD value significantly decreased in CC and CG regions of SRS-D group, compared with normal group or SRS-ND group. Immunohistostaining results were consistent with LFB results. The positive intensity of myelin basic protein (MBP) were reduced remarkably in CC and CG regions in SRS-D group, compared with normal control group or SRS-ND group. No significant differences were found between SRS-ND and normal group. B. C: Relative quantification of LFB and MBP immunohistostaining is depicted in the bar graphs. The values represent the mean ± SD, * $p < .05$, ** $p < .01$. Scale bar = 100 μm.

NG2 in the white matter of SRS-D animals relative to SRS-ND or normal group animals ($p < .05$, Fig. 5D, E). This indicates that SRS-D rats, but not SRS-ND or normal rats, experienced severe demyelination in the cerebral white matter.

3.4. Olig2 expression was reduced while LINGO-1 expression was elevated in the cerebral white matter of SRS-depressed rats

To explore whether demyelination in SRS-D rats was induced by abnormal regulation of Olig2 and LINGO-1, RT-PCR, western blot analysis, and immunohistostaining were used to analyze their expression in cerebral white matter. RT-PCR revealed significantly decreased expression of *Olig2* mRNA and significantly increased expression of *LINGO-1* mRNA in the CG region of SRS-D animals as compared with normal group ($p < .01$, Fig. 6A, B). Western blot analysis confirmed this decreased expression of Olig2 and increased expression of LINGO-1 in SRS-D animals ($p < .01$, Fig. 6C, D). Immunofluorescence revealed that the percentage of Olig2-positive cells was significantly reduced in

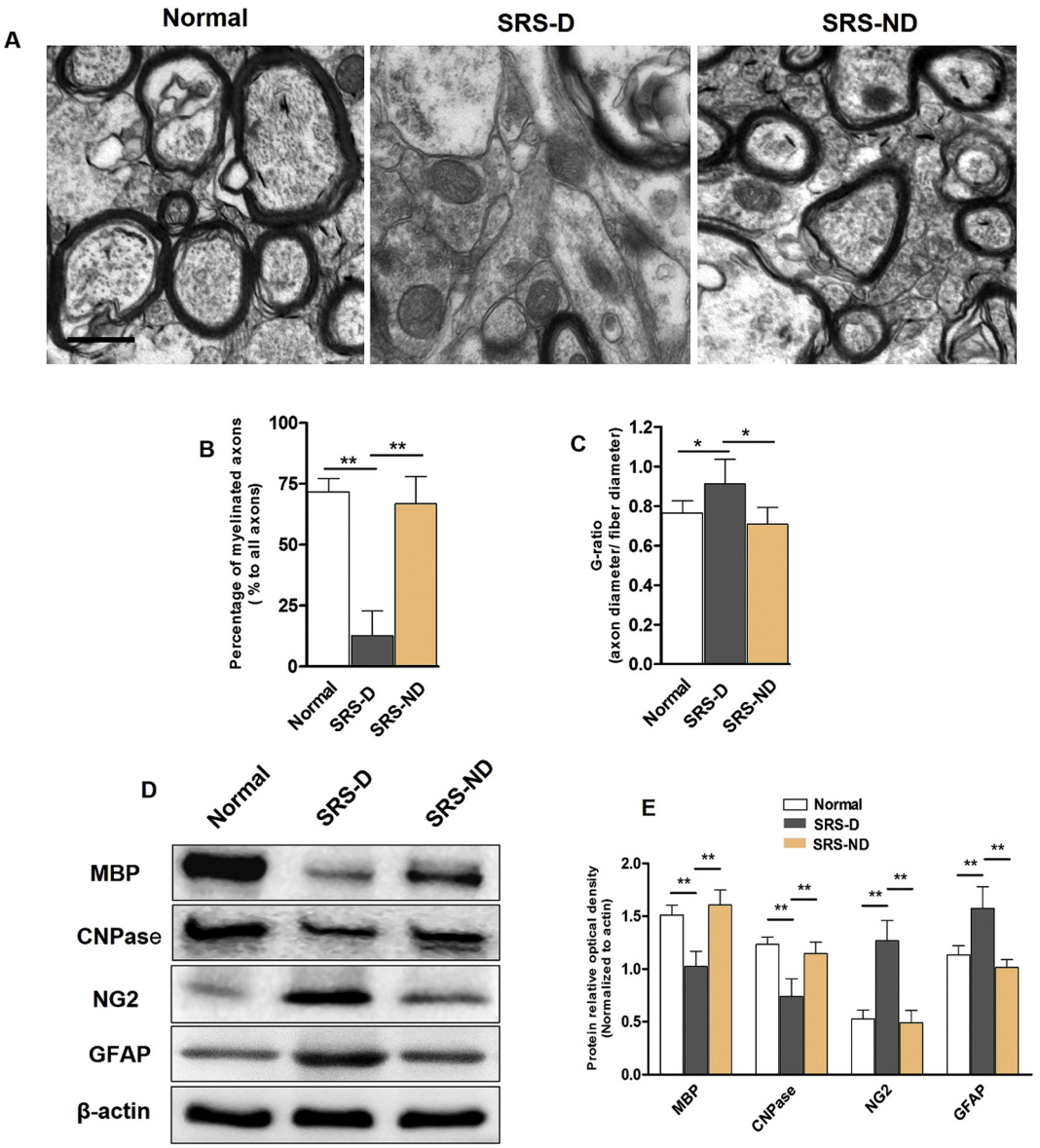

Fig. 5. A: Electron microscopy results showed that SRS-D group presented myelin looseness and thinning compared with normal control group or SRS-ND group. Scale bar = 0.5 μm. B: Percentage of myelinated axons and G-ration (C) of electron microscopy results are depicted in the bar graphs. The values represent the mean ± SD, * $p < .05$, ** $p < .01$. D: Western blot analysis showed the expression of MBP and CNPase proteins were significantly reduced while the expression of GFAP (Astrocytes marker) and NG2 were significantly increased in white matter regions of SRS-D group than that in SRS-ND or normal group. No significant differences were found between SRS-ND and normal control group. E: Relative quantification of western blot results is depicted in the bar graphs. The values represent the mean ± SD, ** $p < .01$.

the CG region of the SRS-D group ($p < .01$, Fig. 6E, G). When compared with normal control group levels, no significant differences in Olig2 expression were found in the CG region of SRS-ND rats ($p > .05$). Additionally, LINGO-1 immunofluorescence revealed low levels of LINGO-1 expression in the CG region but higher levels of MBP expression. In the SRS-D group, LINGO-1 expression was significantly elevated, accompanied by decreased MBP expression ($p < .01$, Fig. 6F, H). In conclusion, these results demonstrate that Olig2 expression was decreased while LINGO-1 expression was elevated in SRS-D rats, resulting in demyelination.

3.5. NCX3 expression was downregulated in the cerebral white matter of SRS-depressed rats

To detect whether demyelination disorders were related to Ca^{2+} signal dysregulation, the expression of NCX3 was assessed in the cerebral white matter of normal control, SRS-D, and SRS-ND group animals. In situ hybridization revealed that *NCX3*-positive signals were observed in CC, CG, and other areas. In the CC and CG, *NCX3* mRNA transcripts were dramatically reduced in the SRS-D group as compared with normal controls ($p < .05$, Fig. 7A, B). Western blot also revealed reduced NCX3 protein optical density in SRS-D animals which coincided with reduced NCX3 mRNA expression ($p < .05$, Fig. 7C, D). However, no significant differences were found via in situ hybridization or western blot analysis between normal and SRS-ND group animals. These results confirm that NCX3 expression is downregulated in the white matter of SRS-D rats.

4. Discussion

Depression and anxiety are the most common comorbidities among patients with severe chronic epilepsy (Hermann et al., 2010; Piazzini

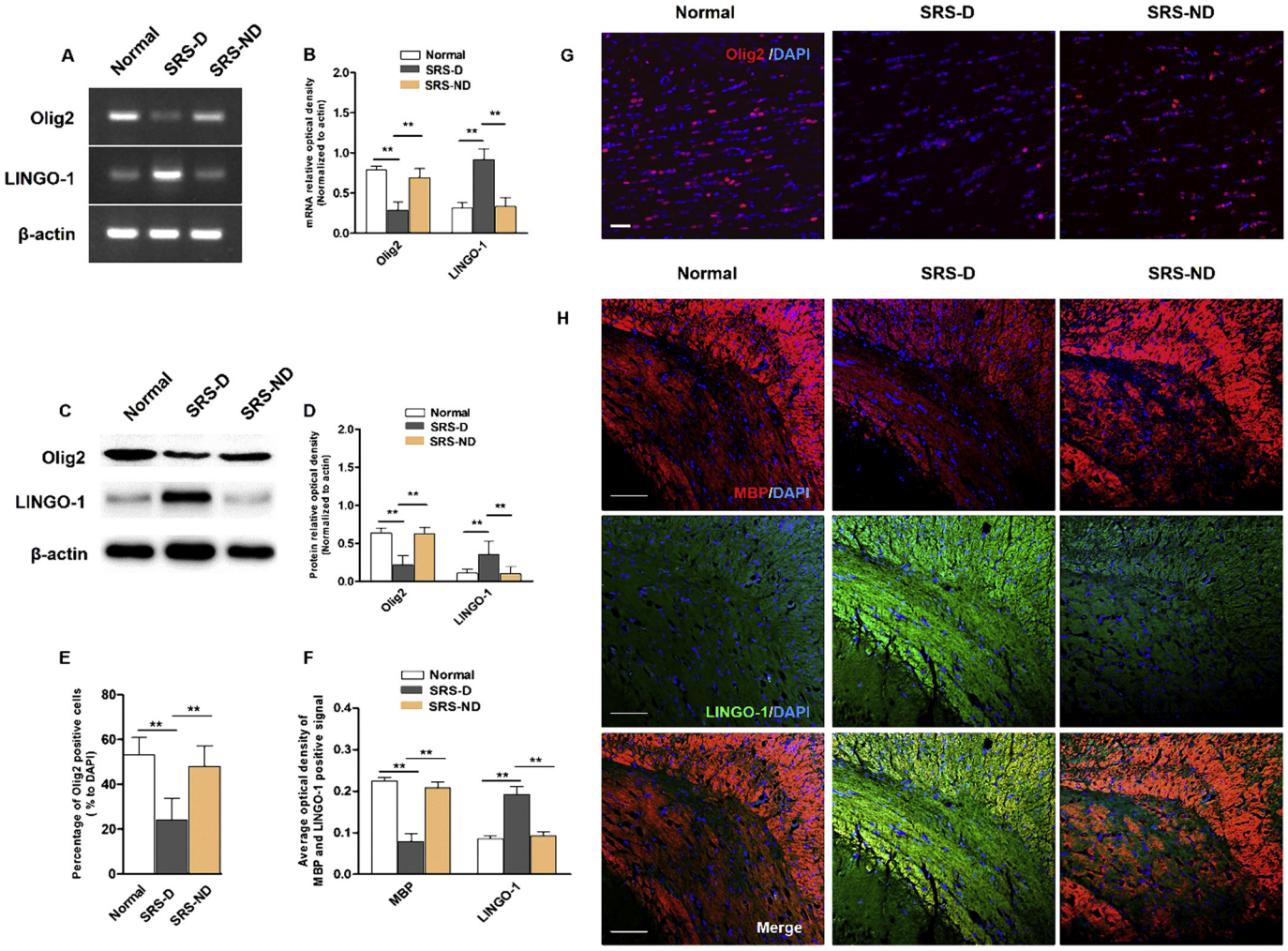

Fig. 6. A: RT-PCR analysis showed significantly decreased expression of *Olig 2* mRNA and significantly increased expression of *LINGO-1* mRNA in CG region of SRS-D group, compared with normal control group or SRS-ND group. B: Relative quantification of RT-PCR results is depicted in the bar graphs. C: Western blot analysis also confirmed the decreased expression of Olig2 proteins and increased expression of LINGO-1 proteins in SRS-D group. No significant differences were found between SRS-ND and normal group. D: Relative quantification of western blot results is depicted in the bar graphs. E. F: Relative quantification of Olig2, MBP, LINGO-1 immunohistostaining results is depicted in the bar graphs. G: Immunofluorescence showed that the percentage of Olig 2 positive cells significantly reduced in the CG region of SRS-D group, compared with normal or SRS-ND group. No significant differences were found between SRS-ND and normal group. Scale bar = 25 μm. H: MBP/LINGO-1 immunofluorescence showed that compared with normal or SRS-ND group, LINGO-1 expression (green) was significantly elevated while MBP expression (red) was decreased in CG region of SRS-D group. No significant differences were found between SRS-ND and normal group. Scale bar = 100 μm. The values represent the mean ± SD, ** $p < .01$. (For interpretation of the references to color in this figure legend, the reader is referred to the web version of this article.)

et al., 2001). Furthermore, epidemiological research has shown that the occurrence of depression is tightly correlated with epilepsy. For instance, O'Donoghue, et al. reported that in a group of 309 patients identified at two large primary care practices in the United Kingdom, 33% patients experienced recurrent seizures and a further 23% had epilepsy with comorbid depression (O'Donoghue et al., 1999).

To better understand the relationship between depression and seizures, pilocarpine injection was used to establish SRS in rats. Depression state was induced and evaluated by behavior assay. As the pilocarpine injection in rats always induced long-term anxiety state and the early onset of anxiety state accelerated the initiation of major depression (Fava et al., 2000), it's necessary to evaluate the secondary anxiety situations 12 weeks after pilocarpine injection. In EPM test, 47% SRS-EPM$^+$ exhibited significantly decreased open arm time and decreased percentage of open arm entries. However, no significant differences of total entries were found between groups. It indicates behavior alterations were induced by anxiety-like response and motor capability were not affected. Then, FST was performed every 3 d in the following 3 weeks to induce the despair behaviors and psychological stress. FST result displayed that apparent despair behaviors with increased immobility time were successfully established in 50% SRS rats. To avoid the false positive results, we further evaluated depression state by SPT. Result displayed that the crucial depressive symptom, anhedonia, only existed in SRS-EPM$^+$/FST$^+$ group (n = 8), which were diagnosed as SRS-D group (8/32). Compared with normal group, the depression state of the other groups was not severe enough. Thus, the rest SRS rats were distributed to SRS-ND group (24/32). It suggests that the existence of anxiety state in pilocarpine-induced SRS rats accelerated the initiation of comorbid depression. It was consistent with clinical studies that anxiety state deteriorated depressive symptoms and interfered depression prognosis (Gaspersz et al., 2017).

For years, clinical research has suggested that the occurrence of depression in patients with epilepsy may be related to their long-term use of antiepileptic drugs (Gómez et al., 2012). However, in the present study, we find a similar comorbidity rate without antiepileptic drug use, suggesting that the application of antiepileptic drugs is not the main cause of depression or its pathogenesis in these patients. Research further has found that both patients with epilepsy and those with

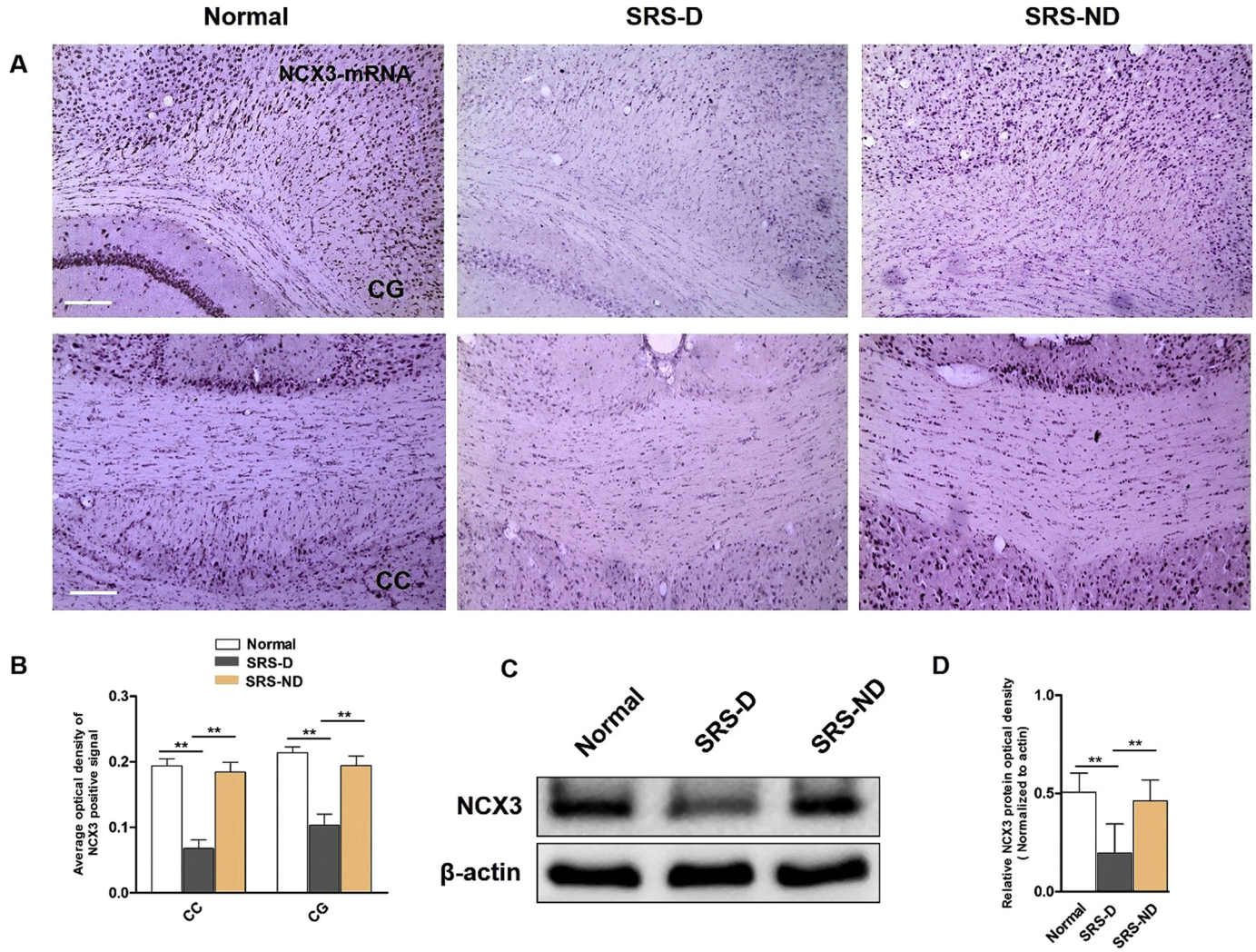

Fig. 7. A: In situ hybridization revealed that *NCX3* positive signals (blue) were dramatically reduced in SRS-D group, compared with normal control or SRS-ND group. No significant differences were found between SRS-ND and normal group. Scale bar = 100 μm. B: Relative quantification of in situ hybridization results is depicted in the bar graphs. C: western blot analysis also presented reduced NCX3 protein optical density in SRS-D group, compared with normal control or SRS-ND group. D: Relative quantification of western blot results is depicted in the bar graphs. The values represent the mean ± SD, ** $p < .01$. (For interpretation of the references to color in this figure legend, the reader is referred to the web version of this article.)

depression exhibit similar structural changes in the cerebral white matter. The brain tissue from epileptogenic focus resection showed decreased formation of myelin sheath and focal depigmentation (Hu et al., 2016). Additionally, early postmortem studies of depression patients have reported decreased oligodendrocytes density in white matter regions critical to major depressive disorders (Tham et al., 2011). Together, these data suggest significant alterations in myelination among patients with both epilepsy and depression.

Myelination disorders may contribute both to the initiation of psychiatric disease and to cognition interference that occurs with ongoing disease. In the present study, we found that SRS-D group animals had significantly reduced MBP expression in the cerebral white matter. Electron microscopy further revealed dysplastic myelination among SRS-D group animals. Additionally, western blot demonstrated decreased expression of MBP and CNPase proteins but increased GFAP and NG2 proteins in the SRS-D group. These data suggest that the development of OLs in SRS-D rats is inhibited and that OLs mostly remain at an immature stage in these animals. In light of the research discussed above, demyelination may contribute to epilepsy-depression comorbidity and is likely absent in simple epilepsy.

Myelination is one of the important features of brain maturation and normal brain function. Normal myelination in the CNS refers to processes of OL migration, differentiation, myelin formation, and its wrapping around axons (Lee et al., 2012). Furthermore, the development of myelin is coordinated with the differentiation of OLs. Thus, myelination processes are always regulated by multiple factors which can affect OL differentiation or myelin protein formation.

In recent years, the functions of Olig2 and LINGO-1 in the regulation of myelination have captured the field's attention. Olig2 has an irreplaceable, promoting effect on the directional differentiation of OLs. For instance, transplantation of Olig2-positive neural stem cells into an injured spinal cord induced a significant increase in the thickness of recovered myelin sheath (Tan et al., 2017). Olig2 accelerates the maturation of OL myelin and promotes the regeneration of the myelin sheath. Here, we report a reduction in Olig2 expression in the CG region of SRS-D animals, suggesting that Olig2 dysregulation is involved in the demyelination that occurs with (and may underlie) epilepsy-depression comorbidity.

While the physiologic expression of Olig2 always decreases after the occurrence of rapid postnatal myelination, typically by postnatal 20 d, the downregulation of Olig2 may also be induced physiologically by discrete factors. The expression of myelination inhibition factor LINGO-1, which is changed in SRS-D rats, is one such factor (Mi et al., 2005). In normal myelination, LINGO-1 expression remains low. However, in

spinal cord injury, LINGO-1 mRNA is elevated to five times its normal levels within 2 weeks, resulting in inhibited remyelination (Mi et al., 2004). These results suggest that LINGO-1 exerts an opposing effect on Olig2's role in myelination and remyelination. In the present study, our results show a significant increase in LINGO-1 in the CG regions as well as decreased MBP expression. Together, these results suggest that abnormal regulation of Olig2 and LINGO-1 in the cerebral white matter was induced pathologically in the SRS-D rats assessed here. Down-regulation of Olig2 significantly inhibited myelination, as did the up-regulation of LINGO-1. This same dysregulation pattern is also implicated in a zebrafish myelination model (Yin and Hu, 2014).

Ca^{2+} signals play a crucial role in OL formation, especially in the early stages of OL development (Takeda et al., 2010). However, the over-accumulation of intracellular Ca^{2+} induced OL injuries and inhibits OL differentiation. Studies have shown that seizures aggravate cerebral hypoxic-ischemic damage and produce oxidative stress, which influences the expression of Ca^{2+} extrusion proteins (Wirrell et al., 2001). For instance, NCX (three isoforms are found in mammals: NCX1, NCX2, and NCX3), a Ca^{2+} extrusion protein located on the plasma membrane, regulates levels of intracellular Ca^{2+} to avoid Ca^{2+} overload. Boscia et al. reported that silencing NCX3, but not NCX1 or NCX2, impaired OLs differentiation (Boscia et al., 2012). Thus, dysregulation of NCX3 may be a hallmark of Ca^{2+} homeostasis disturbance and OL injury. These results demonstrate that NCX3 expression is decreased in our SRS-D group, a pattern that was accompanied by decreased myelination following pilocarpine treatment. Collectively, these data provide evidence that the dysregulation of NCX3-mediated Ca^{2+} signal during OL development and myelin formation is involved in the initiation of demyelination-induced psychiatric disorders and especially in epilepsy-depression comorbidity.

These molecular mechanisms drew a comprehensive picture of demyelination initiation in comorbid depression. The dysregulation of Olig2/LINGO-1 inhibited OL's differentiation while disturbance of Ca^{2+} homeostasis induced injuries in developing OLs, resulting in the inhibited formation of new myelin proteins. These alterations were associated tightly with depression state, but not the anxiety state induced by pilocarpine. As the anxiety-positive rats also existed in SRS-ND group, but severe demyelination only existed in SRS-D group. Additionally, no significant differences of epilepsy severity were found between SRS-D and SRS-ND group. It supports that the severity of depression was the crucial factor associated with demyelination phenotypes and demyelination in epilepsy contributed to the initiation of comorbid depression.

In conclusion, the results of the present study revealed that depression was evident in approximately one quarter of induced-epilepsy rats. This initiation of depression in epilepsy was not caused by the application of antiepileptic drugs, but was strongly associated with demyelination disorder. The dysregulation of Olig2/LINGO-1 and disturbance of Ca^{2+} homeostasis may serve as key molecular mechanism underlying this demyelination and epilepsy-depression comorbidity. The present study also provides morphological and molecular evidence for myelination abnormalities in the cerebral white matter in cases of depression comorbidity. It also provides clinical instructions that the interference of demyelination in the early stage of epilepsy may improve its prognosis.

For further studies, we may try to demonstrate a causal relationship between the dysregulation of molecular signals and the initiation of demyelination, and whether Olig2, LINGO-1 or NCX3 might serve as treatment targets for depression comorbidity. Additionally, the sexual and hormone factors may also play an influential role in depression and their effects need further clarification.

Declaration of Competing Interest

None.

Acknowledgements

This work was supported by grants from the National Natural Science Foundation of China (NSCF 31471148); Natural Science Foundation Project of Chongqing (No. 2010BB5031); Startup Funds Project for Returnee of Third Military Medical University (No. 2011XHG01).

References

Aston, C., Jiang, L., Sokolov, B., 2005. Transcriptional profiling reveals evidence for signaling and oligodendroglial abnormalities in the temporal cortex from patients with major depressive disorder. Mol. Psychiatry 10, 309–322.
Barabas, G., Matthews, W., 1988. Barbiturate anticonvulsants as a cause of severe depression. Pediatrics 82, 284–285.
Baumann, N., Phamdinh, D., 2001. Biology of oligodendrocyte and myelin in the mammalian central nervous system. Physiol. Rev. 81, 871–927.
Benner, B., Martorell, A., Mahadevan, P., Najm, F., Tesar, P., Freundt, E., 2016. Depletion of Olig2 in oligodendrocyte progenitor cells infected by Theiler's murine encephalomyelitis virus. J. Neuro-Oncol. 22, 336–348.
Boscia, F., D'Avanzo, C., Pannaccione, A., Secondo, A., Casamassa, A., Formisano, L., Guida, N., Sokolow, S., Herchuelz, A., Annunziato, L., 2012. Silencing or knocking out the Na+/Ca2+ exchanger-3 (NCX3) impairs oligodendrocyte differentiation. Cell Death Differ. 19, 562–572.
Duarte, F., Duzzioni, M., Hoeller, A., Silva, N., Ern, A., Piermartiri, T., Tasca, C., Gavioli, E., Lemos, T., Carobrez, A., De Lima, T., 2013. Anxiogenic-like profile of Wistar adult rats based on the pilocarpine model: an animal model for trait anxiety? Psychopharmacology 227, 209–219.
Faure, J., Akimana, G., Carneiro, J., Cosquer, B., Ferrandon, A., Geiger, K., Koning, E., Penazzi, L., Cassel, J., Nehlig, A., 2013. A comprehensive behavioral evaluation in the lithium-pilocarpine model in rats: effects of carisbamate administration during status epilepticus. Epilepsia 54, 1203–1213.
Fava, M., Rankin, M., Wright, E., Alpert, J., Nierenberg, A., Pava, J., Rosenbaum, J., 2000. Anxiety disorders in major depression. Compr. Psychiatry 41, 97–102.
Gaspersz, R., Lamers, F., Kent, J., Beekman, A., Smit, J., Hemert, A., Schoevers, R., Penninx, B., 2017. Anxious distress predicts subsequent treatment outcome and side effects in depressed patients starting antidepressant treatment. J. Psychiatr. Res. 84, 41–48.
Gómez, A., Crail, M., López, Z., Martínez, J., 2012. Severity of anxiety and depression are related to a higher perception of adverse effects of antiepileptic drugs. Seizure-Eur J Epilep 21, 588–594.
Hae-Chul, P., Amit, M., Richardson, J., Bruce, A., 2015. olig2 is required for zebrafish primary motor neuron and oligodendrocyte development. Dev. Biol. 248, 356–368.
Harden, C., 2002. The co-morbidity of depression and epilepsy: epidemiology, etiology, and treatment. Neurology 59, S48.
Hermann, B., Seidenberg, M., Bell, B., 2010. Psychiatric comorbidity in chronic epilepsy: identification, consequences, and treatment of major depression. Epilepsia 41, S31–S41.
Hu, X., Wang, J., Gu, R., Qu, H., Li, M., Chen, L., Liu, R., Yuan, P., 2016. The relationship between the occurrence of intractable epilepsy with glial cells and myelin sheath-an experimental study. Eur. Rev. Med. Pharmacol. Sci. 20, 4516–4524.
Jepson, S., Vought, B., Gross, C., Gan, L., Austen, D., Frantz, J., Zwahlen, J., Lowe, D., Markland, W., Krauss, R., 2012. LINGO-1, a transmembrane signaling protein, inhibits oligodendrocyte differentiation and myelination through intercellular self-interactions. J. Biol. Chem. 287, 22184–22195.
Kanner, A., 2003. Depression in epilepsy: prevalence, clinical semiology, pathogenic mechanisms, and treatment. Biol. Psychiatry 54, 388–398.
Kanner, A., Schachter, S., Barry, J., Hesdorffer, D., Mula, M., Trimble, M., Hermann, B., Ettinger, A., Dunn, D., Caplan, R., 2012. Depression and epilepsy: epidemiologic and neurobiologic perspectives that may explain their high comorbid occurrence. Epilepsy Behav. 24, 156–168.
Kavanaugh, B., Correia, S., Jones, J., Blum, A., LaFrance, W., Davis, J., 2017. White matter integrity correlates with depressive symptomatology in temporal lobe epilepsy. Epilepsy Behav. 77, 99–105.
Kip, S., Strehler, E., 2007. Rapid downregulation of NCX and PMCA in hippocampal neurons following H2O2 oxidative stress. Annals of the New York Academy of Sciences 1099, 436–439.
Lee, X., Yang, Z., Shao, Z., Rosenberg, S., Levesque, M., Pepinsky, R., Qiu, M., Miller, R., Chan, J., Mi, S., 2007. NGF regulates the expression of axonal LINGO-1 to inhibit oligodendrocyte differentiation and myelination. J. Neurosci. 27, 220–225.
Lee, S., Leach, M., Redmond, S., Chong, S., Mellon, S., Tuck, S., Feng, Z., Corey, J., Chan, J., 2012. A culture system to study oligodendrocyte myelination-processes using engineered nanofibers. Nat. Methods 9, 917–922.
Ligon, K., Kesari, S., Kitada, M., Sun, T., Arnett, H., Alberta, J., Anderson, D., Stiles, C., Rowitch, D., 2006. Development of NG2 neural progenitor cells requires Olig gene function. PNAS 103, 7853–7858.
Llorens, F., Gil, V., Iraola, S., Carimtodd, L., Martí, E., Estivill, X., Soriano, E., Del, J., Sumoy, L., 2010. Developmental analysis of Lingo-1/Lern1 protein expression in the mouse brain: interaction of its intracellular domain with Myt1l. Dev Neurobiol 68, 521–541.
Lopez-Gomez, M., Ramirez-Bermudez, J., Campillo, C., Sosa, A., Espinola, M., Ruiz, I., 2005. Primidone is associated with interictal depression in patients with epilepsy. Epilepsy Behav. 6, 413–416.

Lopresti, A., Maker, G., Hood, S., Drummond, P., 2014. A review of peripheral biomarkers in major depression: the potential of inflammatory and oxidative stress biomarkers. Prog. Neuro-Psychopharmacol. Biol. Psychiatry 48, 102–111.
Ma, T., Wu, X., Cai, Q., Wang, Y., Xiao, L., Tian, Y., Li, H., 2015. Lead poisoning disturbs oligodendrocytes differentiation involved in decreased expression of NCX3 inducing intracellular calcium overload. Int. J. Mol. Sci. 16, 19096–19110.
Mei, F., Wang, H., Liu, S., Niu, J., Wang, L., He, Y., Etxeberria, A., Chan, J., Xiao, L., 2013. Stage-specific deletion of Olig2 conveys opposing functions on differentiation and maturation of oligodendrocytes. J. Neurosci. 33, 8454–8462.
Mendez, M., Cummings, J., Benson, D., 1986. Depression in epilepsy. Significance and phenomenology. Arch. Neurol. 43, 766–770.
Mi, S., Lee, X., Shao, Z., Thill, G., Ji, B., Relton, J., Levesque, M., Allaire, N., Perrin, S., Sands, B., 2004. LINGO-1 is a component of the Nogo-66 receptor/p75 signaling complex. Nat. Neurosci. 7, 221–228.
Mi, S., Miller, R., Lee, X., Scott, M., Shulagmorskaya, S., Shao, Z., Chang, J., Thill, G., Levesque, M., Zhang, M., 2005. LINGO-1 negatively regulates myelination by oligodendrocytes. Nat. Neurosci. 8, 745–751.
Mi, S., Blake, P., Cadavid, D., 2013. Blocking LINGO-1 as a therapy to promote CNS repair: from concept to the clinic. Cns Drugs 27, 493–503.
O'Donoghue, M., Goodridge, D., Redhead, K., Sander, J., Duncan, J., 1999. Assessing the psychosocial consequences of epilepsy: a community-based study. Br. J. Gen. Pract. 49, 211–214.
Piazzini, A., Canevini, M., Maggiori, G., Canger, R., 2001. Depression and anxiety in patients with epilepsy. Epilepsy Behav. 2, 481–489.
Porsolt, R., Brossard, G., Hautbois, C., Roux, S., 2011. Rodent models of depression: forced swimming and tail suspension behavioral despair tests in rats and mice. Curr Protoc Neurosci 10A Chapter 8, Unit 8.
Racine, R., Okujava, V., Chipashvili, S., 1972. Modification of seizure activity by electrical stimulation: III. Motor seizure. Electroencephalogr. Clin. Neurophysiol. 32, 295–299.
Rajkowska, G., Mahajan, G., Maciag, D., Sathyanesan, M., Iyo, A., Moulana, M., Kyle, P., Woolverton, W., Miguel-Hidalgo, J., Stockmeier, C., Newton, S., 2015. Oligodendrocyte morphometry and expression of myelin - related mRNA in ventral prefrontal white matter in major depressive disorder. J. Psychiatr. Res. 65, 53–62.
Schaerenwiemers, N., Gerfinmoser, A., 1993. A single protocol to detect transcripts of various types and expression levels in neural tissue and cultured cells: in situ hybridization using digoxigenin-labelled cRNA probes. Histochemistry 100, 431–440.
Schaffer, A., Levitt, A., Bagby, R., Kennedy, S., Levitan, R., Joffe, R., 2000. Suicidal ideation in major depression: sex differences and impact of comorbid anxiety. Can. J. Psychiatry 45, 822–826.
Soliven, B., 2001. Calcium signalling in cells of oligodendroglial lineage. Microsc. Res. Tech. 52, 672–679.
Szebeni, A., Szebeni, K., Diperi, T., Chandley, M., Crawford, J., Stockmeier, C., Ordway, G., 2014. Shortened telomere length in white matter oligodendrocytes in major depression: potential role of oxidative stress. Int. J. Neuropsychopharmacol. 17, 1579–1589.
Takeda, M., Nelson, D., Soliven, B., 2010. Calcium signaling in cultured rat oligodendrocytes. Glia 14, 225–236.
Tan, B., Jiang, L., Liu, L., Yin, Y., Luo, Z., Long, Z., Li, S., Yu, L., Wu, Y., Liu, Y., 2017. Local injection of Lenti-Olig2 at lesion site promotes functional recovery of spinal cord injury in rats. Cns Neurosci Ther 23, 475–487.
Tham, M., Woon, P., Sum, M., Lee, T., Sim, K., 2011. White matter abnormalities in major depression: evidence from post-mortem, neuroimaging and genetic studies. J. Affect. Disord. 132, 26–36.
Valente, K., Busatto, F., 2013. Depression and temporal lobe epilepsy represent an epiphenomenon sharing similar neural networks: clinical and brain structural evidences. Arq. Neuropsiquiatr. 71, 183–190.
Wirrell, E., Armstrong, E., Osman, L., Yager, J., 2001. Prolonged seizures exacerbate perinatal hypoxic-ischemic brain damage. Pediatr. Res. 50, 445–454.
Yin, W., Hu, B., 2014. Knockdown of Lingo1b protein promotes myelination and oligodendrocyte differentiation in zebrafish. Exp. Neurol. 251, 72–83.
Yu, Y., Chen, Y., Kim, B., Wang, H., Zhao, C., He, X., Liu, L., Liu, W., Wu, L., Mao, M., 2013. Olig2 targets chromatin remodelers to enhancers to initiate Oligodendrocyte differentiation. Cell 152, 248–261.
Yuen, T., Silbereis, J., Griveau, A., Chang, S., 2014. Oligodendrocyte-encoded HIF function couples postnatal myelination and white matter angiogenesis. Cell 158, 383–396.